

Internalisation and toxicity of amyloid- β 1-42 are influenced by its conformation and assembly state rather than size

Devkee M. Vadukul^{1,2}, Mahmoud Maina^{1,3} , Hannah Franklin¹, Astrid Nardecchia¹, Louise C. Serpell¹ and Karen E. Marshall¹ 

¹ Dementia Research group, Sussex Neuroscience, School of Life Sciences, University of Sussex, Falmer, E Sussex, UK

² CEMO-Alzheimer Dementia group, Institute of Neuroscience, Université catholique de Louvain, Brussels, Belgium

³ College of Medical Sciences, Yobe State University, Nigeria

Correspondence

K. E. Marshall, Dementia Research group,
Sussex Neuroscience, School of Life
Sciences, University of Sussex, Falmer,
E Sussex, UK
Email: K.E.Marshall@sussex.ac.uk

(Received 23 June 2020, revised 30 July
2020, accepted 19 August 2020, available
online 11 September 2020)

doi:10.1002/1873-3468.13919

Edited by Barry Halliwell

Amyloid fibrils found in plaques in Alzheimer's disease (AD) brains are composed of amyloid- β peptides. Oligomeric amyloid- β 1-42 (A β 42) is thought to play a critical role in neurodegeneration in AD. Here, we determine how size and conformation affect neurotoxicity and internalisation of A β 42 assemblies using biophysical methods, immunoblotting, toxicity assays and live-cell imaging. We report significant cytotoxicity of A β 42 oligomers and their internalisation into neurons. In contrast, A β 42 fibrils show reduced internalisation and no toxicity. Sonication of A β 42 fibrils generates species similar in size to oligomers but remains nontoxic. The results suggest that A β 42 oligomers have unique properties that underlie their neurotoxic potential. Furthermore, we show that incubating cells with A β 42 oligomers for 24 h is sufficient to trigger irreversible neurotoxicity.

Keywords: Alzheimer's disease; amyloid fibril; neurotoxicity; oligomer

A key pathological hallmark of Alzheimer's disease (AD) is the deposition of extracellular amyloid plaques in the brain [1]. Plaque deposits in AD brains are composed of self-assembled forms of the amyloid- β (A β) peptide arranged into cross- β amyloid fibrils [2–4]. The A β 42 peptide isoform is one of the primary components of these amyloid plaques. A β 42 self-assembly in vitro involves the formation of oligomers, protofibrils and mature fibrils. This process has been shown to occur via nucleated polymerisation, and intermediates are thought to be critical in cytotoxicity [5–8]. Characterisation of each of these assembled forms of A β 42 has been extensive. For example, Bitan et al. showed the preferential formation of A β 42 pentamer/hexamers in the initial stages

of oligomerisation which elongate to form protofibrils [9,10]. Protofibrils have been defined as being prefibrillar, curvy linear assemblies < 200 nm in length [11] that lead to formation of amyloid fibrils. Mature amyloid fibrils are insoluble rod-like assemblies characterised by the cross- β structure, which is attributed to the orientation of β -strands running perpendicular to the fibre axis, with pairs of β -sheets being tightly associated via interdigitating amino acid side chains [12]. Cryo-electron microscopy (cryo-EM) and solid-state nuclear magnetic resonance (ssNMR) have provided atomic structures of A β 42 fibrils confirming a parallel, in-register cross- β structure characteristic of amyloid [13–18]. Amyloid fibrils are thought to play a role in AD due to the dystrophic

Abbreviations

AD, Alzheimer's disease; A β , amyloid- β ; BME, β -mercaptoethanol; CD, circular dichroism; cryo-EM, cryo-electron microscopy; DMSO, dimethyl sulfoxide; HRP, horseradish peroxidase; ssNMR, solid-state nuclear magnetic resonance; TEM, transmission electron microscopy.

neurons, activated microglia and reactive astrocytes surrounding plaque areas [19,20].

Small, prefibrillar oligomeric species of the A β 42 peptide have been identified as the primary culprits of toxicity [2,21–23]. Focus on these assemblies has been heavily influenced by the correlation between cognitive decline and soluble A β [23]. The term ‘oligomer’ covers a large range of sizes, leading to arguments for different sizes being more or less toxic than others. Several A β 42 oligomeric assemblies have been identified as cytotoxic [2,5,24–31]. A β 42 oligomers have been shown to cause receptor-mediated cytotoxicity [21], permeation of biomimetic membranes [8,32,33], changes in lysosomal pathways [34–37], disruption of cellular homeostasis through intracellular accumulation of A β 42 oligomers [38,39], and oxidative stress induction and protein synthesis impairment [40]. Additionally, A β fibrils have been implicated as reservoirs of oligomers, facilitating further toxicity [23,41–43]. However, the properties that confer cytotoxicity and the mechanisms by which they lead to neurodegeneration have not been fully established.

Here, the importance of structure, size and assembly state of A β 42 on toxicity and internalisation into hippocampal neurons was assessed by comparing A β 42 oligomers (A β O) [44] with mature (A β F) and sonicated A β 42 fibrils (A β Son). A β O and A β F were obtained by incubating monomeric A β 42 at room temperature for 2 and 48 h, respectively. Sonication of mature fibrils results in assemblies that approximately correspond to the size of oligomers and protofibrils. We show that sonicated fibrils retain structural characteristics of mature fibrils, whereas the oligomer samples are in the early stages of self-assembly. Only A β O were toxic and internalised significantly more than A β Son or A β F. Our results suggest that assembly size alone does not determine toxicity and does not correlate directly with internalisation. We propose that A β O have unique characteristics that might enhance their ability to be internalised and contribute to their toxicity. We have also identified a threshold of A β O exposure/internalisation after which the cell can no longer recover and significant oligomer-induced cytotoxicity is displayed.

Results

Sonication of fibrils results in species with a similar size to oligomers, but a similar conformation to fibrils

A β 42 peptide was pretreated to remove preaggregated species and solvent contaminants then incubated for

2 h to generate oligomers or 48 h to produce a predominantly fibrillar sample. Oligomer preparation was based on a previously optimised protocol [44]. The fibrillar sample was sonicated to produce small species, referred to as oligomer-like, similar in size to A β O. Although sonicated fibrils are unlikely to elongate by primary nucleation due to a depleted pool of monomer, sonication was carried out on ice to prevent the possibility of further assembly by secondary nucleation [45,46]. Fibrils were sonicated for 5, 10 and 20 min to optimise the generation of oligomer-like species (Fig. 1A). Five minutes was not sufficient to fragment the fibrils, whereas by 20 min no species were present by transmission electron microscopy (TEM; therefore, 10 min was selected as optimal. The particle sizes were measured from TEM images and compared with oligomeric samples (A β O (Fig. 2A) that contained spherical species with diameters ranging from 4.5 to 45 nm. TEM of A β Son shows a distribution of small curvy linear fibrils and small spherical species measuring between 5 and 794 nm in length ($n = 544$) (Fig. 1B). 90% were ≤ 200 nm, and 50% were ≤ 45 nm. The diameters of A β Son species ranged from 7 to 50.5 nm (Fig. 1C). Comparisons of A β O with A β Son showed both had a median diameter size of ~ 20 nm for both oligomer and oligomer-like species formed by sonication (Fig. 1D). Combined, these results show that sonicating A β fibrils produces species that are comparable in size to A β oligomers.

Transmission electron microscopy was used to compare oligomeric, fibrillar and sonicated fibril morphologies (Fig. 2A). The conformation of A β O, A β F and A β Son was investigated further using circular dichroism (CD) in combination with western blotting. The CD spectrum for A β O shows a minimum at ~ 198 nm and a second shoulder at ~ 220 nm, suggesting that the solution contains random coil conformation with a contribution of β -sheet (Fig. 2B, blue line). We have previously shown that freshly prepared A β 1–42 is entirely random coil, that is with no signal at 220 nm following dissolution and develops over-time to show increasing β -sheet content [44]. A β F and A β Son show similar spectra with minima at ~ 218 nm and maxima at ~ 198 nm consistent with β -sheet structure (Fig. 2B, black and red lines, respectively). The A β Son minimum has an increased intensity consistent with increased solubility of the smaller species. This suggests that at the secondary structural level, the oligomeric sample is either a mixture of species in solution (unaggregated, monomeric peptide generating a random coil signal and β -sheet-rich oligomers), or oligomers that contain both random coil and β -sheet conformation. Nevertheless, it is likely that the

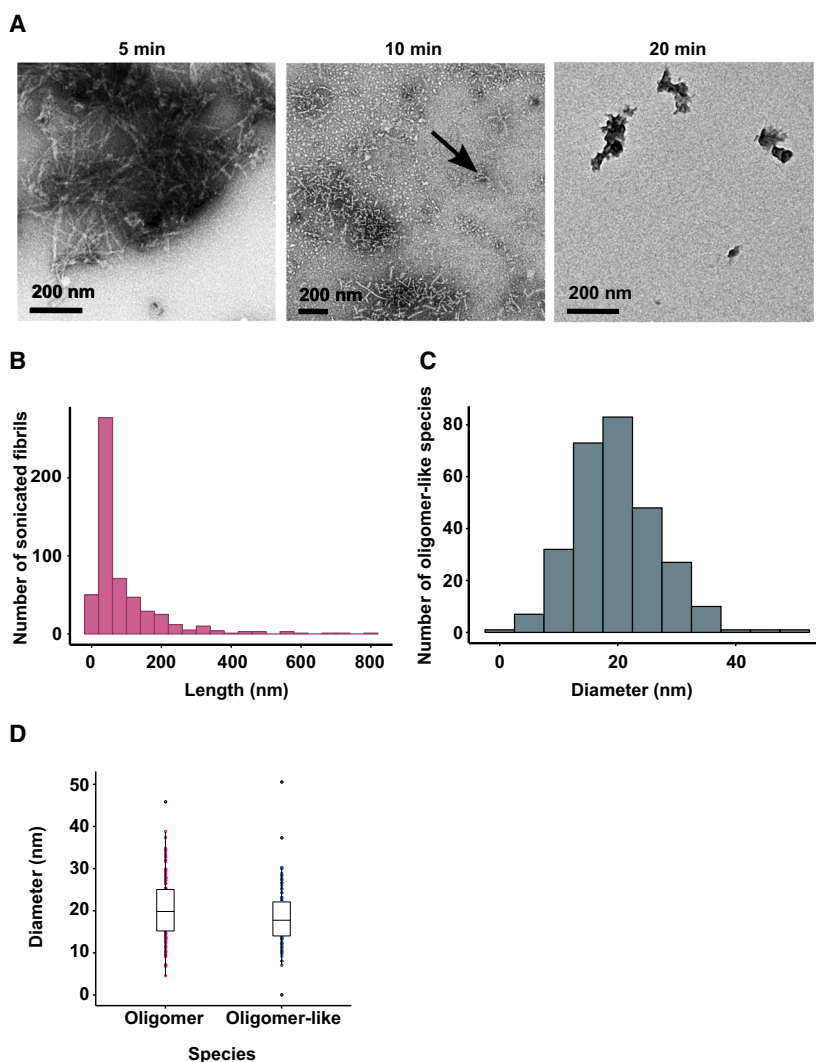


Fig. 1. Optimisation of A β 42 fibril sonication (A β Son). (A) A β 42 fibres were sonicated at the maximum setting for 5, 10 and 20 min on ice. 10 min of sonication was selected as the optimal time for the generation of oligomer-like species (black arrow). Measurement and quantification of the length (B) and diameter (C) of oligomer-like A β 42-sonicated fibres ($n = 544$) from TEM images. (B) Lengths ranged from 5 nm to 794 nm, with 90% ≤ 200 nm and 50% ≤ 45 nm, the latter being the maximum A β O diameter measured. (C) Diameters of sonicated fibres ranged from 7 nm to 51 nm. (D) Box plot showing the range of diameters in oligomer and oligomer-like species (median for both = 20 nm). Scale bar = 200 nm. 50 μ M A β 42 was prepared in 10 mM HEPES buffer pH 7.4 and incubated for 48 h at room temperature to obtain a predominantly fibrillar population before sonication.

shoulder at ~ 220 nm is the result of oligomer formation, showing they do have some β -sheet content.

SDS/PAGE with western blotting using the anti-A β antibody 6E10 (Fig. 2C), which recognises the N-terminal residues 4–10 of A β [47], shows that A β O migrates with bands with molecular weights corresponding to monomeric, dimeric and trimeric species with some higher molecular weight species consistent with previous reports [44]. The majority of A β F is found in the well with some higher molecular weight species but showing no lower molecular weight bands. A β Son migrates with a band distribution similar to A β O showing monomeric, dimeric and trimeric species but with higher molecular weight species and some material in the well similar to A β F. This suggests that the A β Son sample is representative of some species similar in size to that of the oligomeric sample.

A β O but not A β F or A β Son is cytotoxic following internalisation

Next, we sought to examine the toxicity of the different A β 42 assembly preparations. The ReadyProbes live/dead assay was used to assess the effect of 10 μ M A β O, A β F and A β Son incubated with primary hippocampal cultures for 72 h (Fig. 3). A β O displayed $43 \pm 2\%$ cell death, whilst A β F and A β Son displayed $18 \pm 2\%$ and $20 \pm 2\%$ cell death, respectively. Only the oligomeric preparation showed significant cell death compared with buffer control. Previous studies have shown that oligomeric A β 42 is internalised into neuroblastoma cells and primary hippocampal neurons [35,37,44,48–53], therefore, we compared the internalisation of the three A β 42 preparations to determine whether the ability to be internalised was linked to toxic potential. A β 42 was tagged with an Alexa Fluor

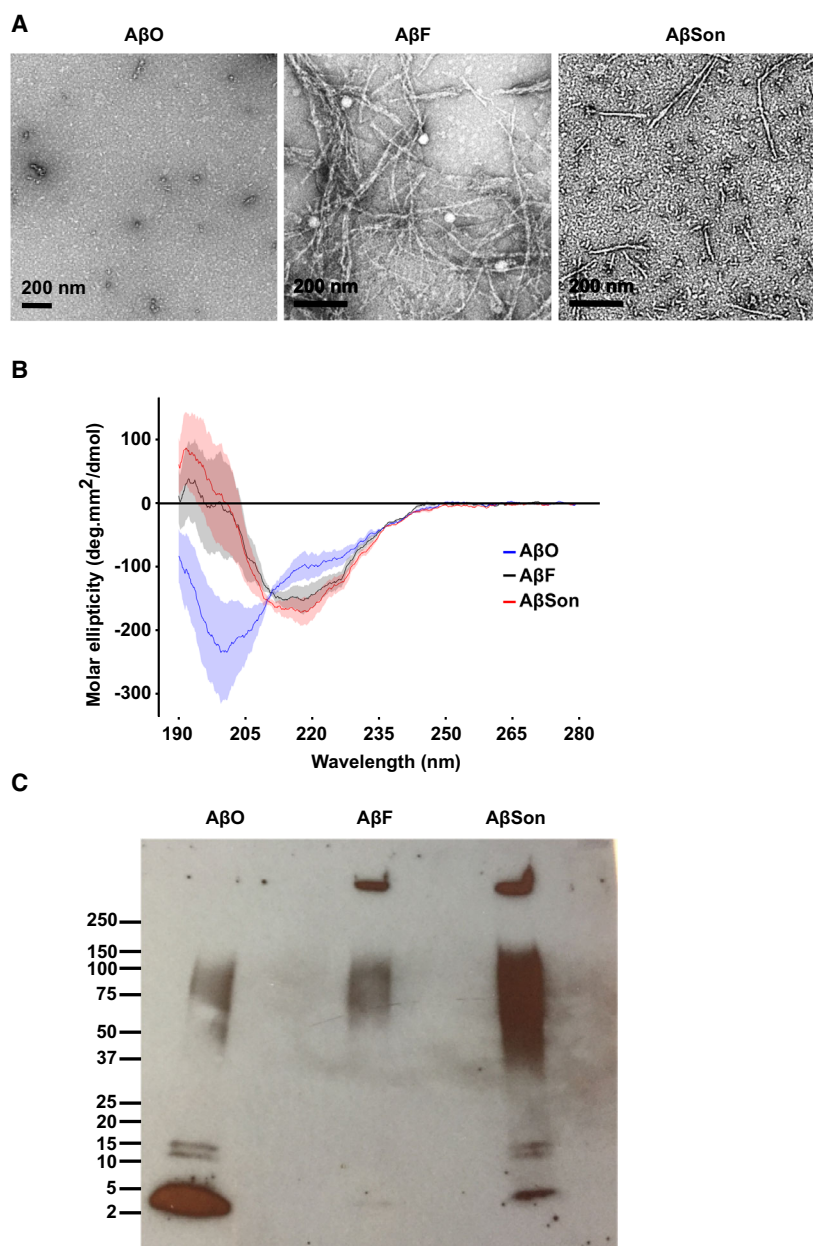


Fig. 2. (A) Negative stain transmission electron micrographs for A β O, A β F and A β Son. Small, spherical assemblies are present in the oligomer preparation, elongated fibrils in the fibrillar preparation and sonicated fibrils contain short fibrils and smaller species. Scale bars are 200 nm. (B) CD spectra for A β O, A β F and A β Son. 50 μ M A β 42 was incubated for 2 h at room temperature for A β O, 48 h for A β F, and these were sonicated on ice for 10 min for A β Son. A β O shows a random coil signal (minimum at -198 nm), and A β F and A β Son show a β -sheet signal (minimum at -218 nm, maximum at -198 nm). Samples were prepared in 20 mM phosphate buffer pH 7.4 and measured in a 1-mm pathlength cuvette. Error bars expressed as \pm SEM, $n = 3$. (C) Western blot of A β O, A β F and A β Son samples using 6E10 to detect the size of assemblies present in each sample. A β O migrate as monomers (4.5 kDa), dimer/trimers (9 kDa/13.5 kDa) and a smear of higher molecular weight species. A β F show no lower molecular weight species with some fibrils stuck in the well of the gel. A β Son show a mixture of all species from monomers to fibrils. Samples were prepared in 10 mM HEPES buffer pH 7.4.

dye that conjugates to amine groups [35,44], and the Alexa Fluor 488-labelled A β O, A β F and A β Son were incubated with neurons for up to 72 h and examined using live-cell imaging after 4-, 24- and 72-h incubation times (Fig. 4). Green puncta were observed within the cell body for all species after 4-h incubation (Fig. 4A, white arrows), and there was no significant difference between the fluorescence intensity in cells treated with either A β O, A β F or A β Son, which have mean intensities of 7 ± 2 , 6 ± 4 and 7 ± 3 AFU, respectively (Fig. 4B). At 24 h, the mean fluorescence intensity in cells treated with A β O increased to

14 ± 8 , compared with 10 ± 4 for A β F and 14 ± 9 AFU for A β Son. The difference between A β Son and A β F is significant. After 72 h, the differences were more pronounced and significantly different from one another, with A β O showing a mean intensity of 31 ± 13 , A β F 10 ± 7 and A β Son 18 ± 13 AFU (Fig. 4B). Although there is a significant difference in fluorescence intensity of A β F and A β Son (Fig. 4B and Fig. S1), there is a larger difference between A β O and A β Son, suggesting that the uptake of sonicated fibrils is less efficient than oligomers. The fluorescence intensity of each species increases over time, indicating that

the cell continues to endocytose A β 42. The results show that neurons preferentially take up oligomeric A β 42 species but can also endocytose fibrillar and sonicated fibrillar species to a lesser degree.

At least 24-hour incubation is required for A β O toxicity

We have shown that A β O is more toxic and more readily internalised than A β Son and A β F. To examine the link between internalisation of A β O and the exposure time required to result in toxicity, the ReadyProbes assay was used to measure cell death after incubation with A β O for 2, 4 or 24 h. A β O was removed from the culture after the specified incubation period and replaced with fresh, A β -free media, thereby removing A β O from the environment. Cell viability was measured 7 days after initial incubation with A β O and presented as a percentage of dead cells in culture (Fig. 5). As the aim of this experiment was to identify whether there is a threshold of A β O exposure after which the cell can no longer recover, this 7-day time point was chosen based on our previously presented work where we have shown a much more pronounced A β O-induced cytotoxicity compared with 3 days. This ensured that any lack of significant cytotoxicity after 3 days was not simply due to a slower rate of cytotoxicity once A β O had been removed from the cellular environment and replaced with fresh media. The cytotoxicity of A β O incubated for the full 7 days was $66 \pm 3\%$. Cells incubated for 2 or 4 h with A β O before being replaced with fresh media displayed no significant cytotoxicity compared with buffer incubated cells, which also had a media change, at 7 days (18% and 26% , respectively). Cells incubated with A β O for 24 h before being exchanged with fresh media displayed significant toxicity at 7 days ($\sim 41 \pm 4\%$). Combining this with the internalisation data, toxicity appears to correlate with the amount of A β O internalised into the cell. Four hours after adding to cells, only a relatively small amount of A β O has been internalised, and there is no toxic effect. A β O are toxic to cells only after incubation at 24 h, when there are increased levels of A β O inside the cell (Fig. 4A). Our findings suggest a threshold is reached between 4 and 24 h, at which point the cells can no longer recover from the amyloid insult. Removing A β O after 2 and 4 h does not allow for this threshold of internalisation to be reached, and no significant toxicity is observed after 7 days.

Discussion

The work presented here aims to assess the importance of size, structure and assembly state of A β 42 on

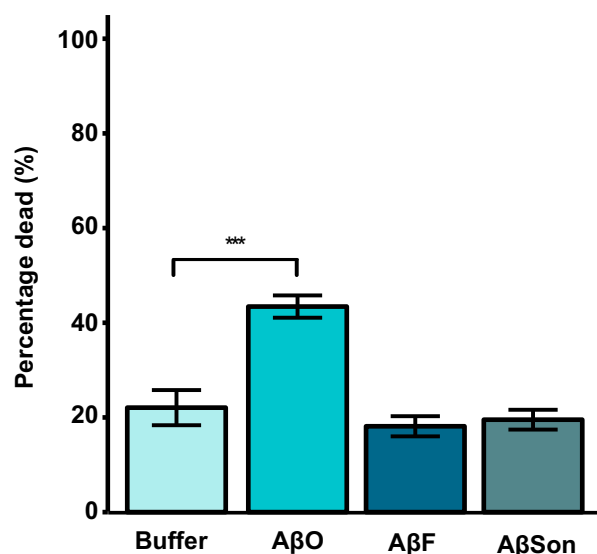


Fig. 3. A β O, A β F and A β Son ReadyProbes cell viability assay. Rat hippocampal cultures were treated with $10 \mu\text{M}$ A β O, A β F and A β Son (prepared in 10 mM HEPES buffer pH 7.4) for 3 days ($n = 3$). Cytotoxicity was measured as a percentage of dead cells in a culture and compared with buffer incubated cells. A β O were significantly toxic ($43 \pm 2\%$, total number of cells = 1619, number of dead cells = 703). A β F ($18 \pm 2\%$, total number of cells = 783, number of dead cells = 142) and A β Son ($20 \pm 2\%$, total number of cells = 425, number of dead cells = 83) showed no significant cytotoxicity compared with buffer incubated cells ($18 \pm 3\%$, total number of cells = 1239, number of dead cells = 221). Unpaired parametric Student's t -test where $P \leq 0.01$ (*), <0.001 (**), <0 (***). Error bars are expressed as \pm SEM.

internalisation and neurotoxicity. We first characterised the conformation and size of A β O, A β F and A β Son. TEM allowed visualisation and measurement of the different species. The ability of sonication to produce species similar to oligomers has been previously shown for hen egg-white lysozyme [54] and the prion protein [55] and has been used to investigate the effect of fibril size on biological activity [56]. Although there was some heterogeneity in length in the sonicated fibril sample, the conditions used did generate approximately half the sample with species that had the same dimensions as the oligomers, with a large majority (90%) being within the range of what could be considered protofibrillar, that is 200 nm [11,57] or smaller.

Although the A β O sample displayed a predominantly random coil conformation by CD, this is likely to arise from remaining monomer in solution dominating the spectra. The western blot shows a dominant SDS-soluble monomer band, although it has been shown that some oligomeric forms of A β 42 can be broken down in the presence of SDS [58–60],

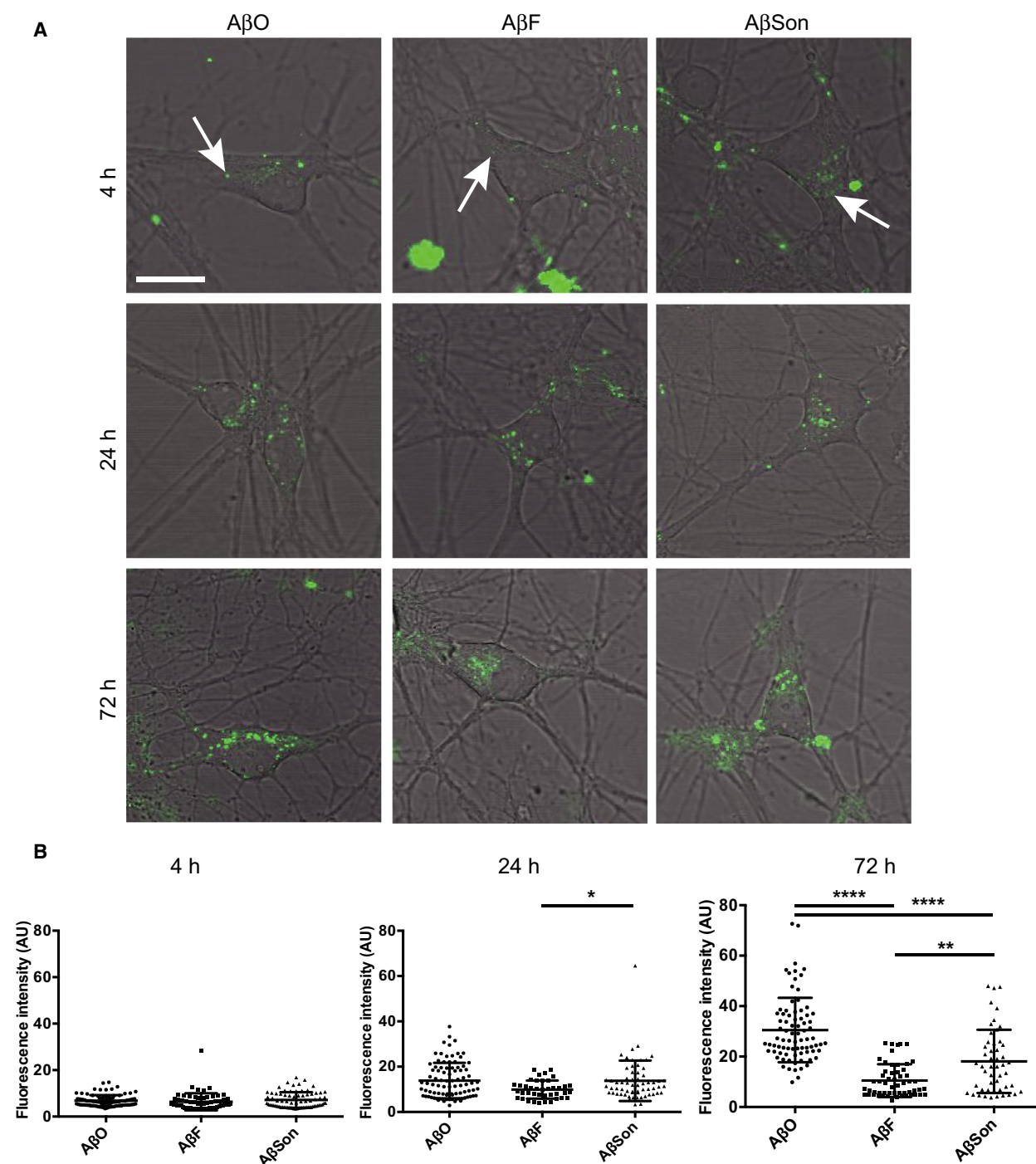


Fig. 4. Internalisation of Alexa Fluor 488-tagged $A\beta O$, $A\beta F$ and $A\beta Son$ in primary hippocampal rat neurons. 10 μM $A\beta O$, $A\beta F$ and $A\beta Son$ were added to cells in culture and imaged at 4, 24 and 72 h. (A) Representative images of cells. Identical lookup tables have been applied across all images. One 0.5- μm z-slice from the middle of the cell body is shown. Scale bar is 20 μm . White arrows indicate green fluorescent intracellular puncta. (B) Quantification of 488 fluorescence intensity from at least three experiments per condition. n (cells) 4 h $A\beta O$ = 91, $A\beta F$ = 63, $A\beta Son$ = 77. 24 h $A\beta O$ = 90, $A\beta F$ = 40, $A\beta Son$ = 62. 72 h $A\beta O$ = 81, $A\beta F$ = 56, $A\beta Son$ = 50. Kruskal–Wallis one-way ANOVA, with Dunn’s multiple comparison test. Only significant differences are shown, * P = 0.05, ** P = 0.005, **** P = 0.0005.

therefore, we do not consider this to be a quantifiable representation of what is in the oligomeric sample. The information provided by CD is an average of the secondary structures within the sample and cannot distinguish between, for example, a sample of pure oligomers with mostly random coil conformation and a mixture of unfolded monomer and β -sheet-rich oligomers. Although we cannot draw any conclusions as to the structure of the oligomers using CD, we can infer from several lines of evidence that they are likely to be transitioning from random coil to a more β -sheet structure. Firstly, there is a contribution of β -sheet in the CD spectra. Secondly, as we have shown previously, this shoulder is not present in solutions of freshly prepared, nonaggregated A β 42 and, importantly, the random coil minimum at 198 nm reduces as

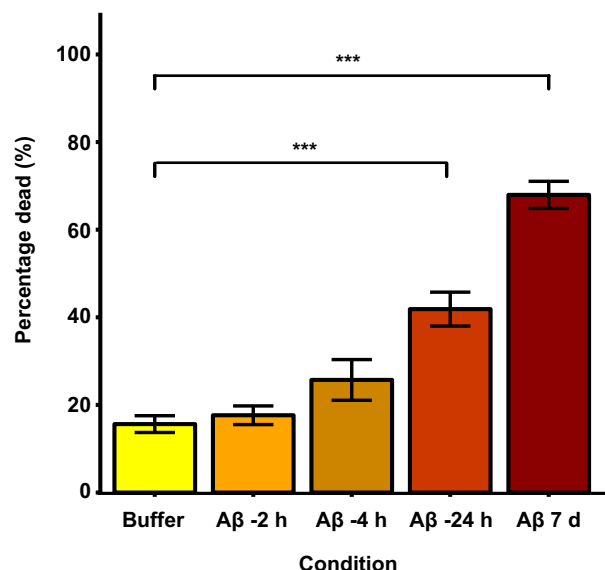


Fig. 5. Cytotoxicity of internalised A β O. Rat hippocampal cultures were treated with 10 μ M A β O (prepared in 10 mM HEPES buffer pH 7.4) for 2, 4 or 24 h before being removed and replaced with A β -free media. Cells were then incubated up to 7 days and then cytotoxicity measured using the ReadyProbes cell viability assay, expressed as a percentage of dead cells and compared with buffer incubated cells, which also had a media change. The percentage of dead cells in buffer control was 16 \pm 2% (total number of cell = 1152, number of dead cells = 180). A β O were significantly toxic (66 \pm 3%, total number of cells = 1172, number of dead cells = 777) at 7 days. Cells incubated with A β O for 2 and 4 h displayed no significant cytotoxicity at 7 days (18 \pm 2%, total number of cells = 595, number of dead cells = 105 and 26 \pm 3%, total number of cells = 599, number of dead cells = 154, respectively). Cells incubated with A β O for 24 h displayed significant cytotoxicity at 7 days (41 \pm 4%, total number of cells = 602, number of dead cells = 249). Unpaired parametric Student's *t*-test where $P \leq 0.01$ (*), < 0.001 (**), < 0 (***). Error bars are expressed as \pm SEM ($n = 3$).

aggregation and oligomer formation proceeds and as monomer is depleted [44]. Finally, many groups have reported that oligomeric species are β -sheet-rich structures [41,61,62]. Therefore, we propose that although A β O shows a dominating random coil signal, this is masking some β -sheet spectra. Both A β F and A β Son display a similar β -sheet-rich conformation by CD. However, only the sonicated fibrils show a wide size range of assemblies detected by western blot, some of which corresponded to the size of A β O. While we do not know the exact conformation of the different oligomeric species revealed by western blot or TEM, we can be confident that by sonicating fibrils we have generated species that are a similar size to oligomers that are not present in the A β F sample, as well as some smaller and larger species.

Fragmented A β 42 fibrils might be expected to retain the cross- β structure present in the mature fibril [63], whereas oligomers formed at early stages of assembly may have a different β -sheet-rich conformation. There is a large body of evidence supporting the formation of β -sheet-rich oligomers and these being structurally distinct from mature fibrils. NMR spectroscopy has shown that neurotoxic oligomers consist of loosely aggregated β -strands arranged as a pentamer that do not have the same β -sheet structure contained within fibrils [58]. ssNMR has revealed oligomers with parallel β -sheets [64,65] and hexameric β -barrels [66]. The formation of β -sheet-rich pore-forming oligomers has also been extensively reported which are folded differently to the cross- β structure of mature amyloid fibrils [67–69]. Furthermore, previous studies have shown a large overlap in the sizes of prefibrillar and fibrillar oligomers [41], suggesting that distinct conformations of the same size exist [70]. In line with this idea, our data suggest that the sonicated oligomer-like species and protofibrils generated by sonication have a high β -sheet content that is most likely structurally similar to mature fibrils. On the other hand, A β O will be more structurally dynamic and still in the process of elongation, so while they most likely contain β -sheet structure it could be distinct to the A β F and A β Son structure. This therefore allows us to test the effects of conformation, size and self-assembly propensity on internalisation and cellular health.

Measuring the cytotoxicity of each species confirmed only A β O were significantly toxic after 3 days, while A β F and A β Son showed no significant cytotoxicity. As around 50% of the A β Son sample is species similar in size to A β O, we might have expected to see at least some toxic effect from the A β Son sample if toxicity were solely mediated by oligomer size. In contrast with our results using fragmented A β 42 fibrils, it has been

previously demonstrated that shortened amyloid fibril length correlates with reduced cellular health [56]. Fragmented amyloid fibrils of β 2-microglobulin, lysozyme and α -synuclein proteins showed increased ability to affect membrane integrity and overall cell viability, likely due to an increased number of toxic fibril-membrane interactions. Their study also highlights the differential response of three cell lines to mature or fragmented fibrils. It is possible that different concentrations and/or incubation times are required in primary neurons to observe similar cellular dysfunction. Therefore, while cytotoxicity may to some extent depend on the physical properties (e.g. length and width) of an amyloid aggregate, our results show that many other factors including peptide precursor (which would in turn determine the molecular structure), cell type and readout of cell viability are all contributing factors in determining the toxic potential of amyloid aggregates *in vitro*. The significant A β 42 oligomer-induced cytotoxicity compared with that displayed by fibrillar A β 42 has been previously demonstrated [71–75]. Furthermore, the presence of dimers and trimers in both A β O and A β SON, which are likely to be similar assemblies, suggests that these alone are not sufficient to cause cytotoxicity as assessed in the timeframe of our experiments. We have shown in previous work that an assembly impaired variant of A β 42 (F20A, G37D) that remains monomeric does not affect cell viability [44], in line with studies showing that the less aggregation-prone A β 40 isoform is significantly less toxic than A β 42 [73].

We and others have previously shown that oligomeric A β 42 is internalised into cells [35,37,44,48,49,51–53]. To study whether this may be linked to toxicity, we examined the internalisation of the different species into primary hippocampal neurons and found that at three days, where we know A β O to be toxic, there was significantly more internalisation than either A β F or A β SON. There is least uptake from the A β F sample and no toxicity, suggesting that smaller species are more readily internalised and that this process leads eventually to cell death. The internalisation of A β SON species was greater than fibrils, perhaps due to an increased number of fibril ends and therefore fibril-membrane interactions that may lead to enhanced internalisation [56,76]. These results indicate a possible correlation between the amount of internalisation and toxicity. Various studies have suggested a link between the accumulation of intracellular A β and neuronal pathology [77–79] although further work is needed to establish a causative link between internalisation and cytotoxicity. Furthermore, we show that oligomers are only toxic after they have been incubated with cells for

24 h and that this effect can be prevented if oligomers are removed before this time. This is consistent with our recently published work showing significant levels of A β O toxicity in hippocampal neurons assessed after 24-hour incubation at the same concentration [35]. Toxicity assessed at 24 h of A β O incubation was roughly half of that seen here where we have removed A β O after 24 h and assessed cytotoxicity at day 7 after initial oligomer addition. This suggests that the downstream effects continue to occur and cause further cytotoxicity even if oligomers are removed from the extracellular environment. Increasingly significant levels of A β O toxicity at 3 and 7 days have also been shown with incubated hippocampal neurons, further supporting the idea that longer oligomer exposure leads to higher toxicity [35,44]. It has been proposed that there is a threshold of oligomer internalisation after which the cell is unable to efficiently clear or degrade A β [80] and therefore no longer recover. Therefore, it is conceivable that if sufficient amounts of A β SON were able to be endocytosed, or if they were left on the cell for long enough, they might also be toxic.

The reduced internalisation of A β SON compared with A β O may explain why the species are not toxic, but why do they show such a significantly reduced uptake? It might be that the reduced internalisation is due to a lower concentration of oligomers of a particular size that are more abundant in the A β O sample. However, this seems unlikely as the majority of species (90%) in the A β SON sample are up to a maximum of 200 nm in length, much shorter than their parent fibrils, which are of indeterminate length in the range of microns. Particle size has shown to be an important determinant in endocytosis with a limit of 200 nm for clathrin-mediated pathways [81,82]. Therefore, it is feasible that comparable levels of A β SON and A β O could be internalised by the cell if the process was solely based on size. Our data clearly show that neurons are able to endocytose assemblies of any size, but to very different extents. Although there were no low molecular weight oligomers in the A β F sample, there was still some uptake. This could be endocytosis of full-length fibrils, fibrils fragmented once inside the cell possibly by the cell membrane, or uptake of oligomers that have dissociated from fibril ends [83]. Previous studies have shown that A β oligomers interact with and disrupt membrane bilayers differently to monomer or fibres. Oligomers extract lipids from the membrane in a detergent-like manner, whereas fibres embed within the bilayer [84]. In addition, only oligomers of A β 42 and not A β 40 are able to form ion channels [85]. Similarly, the oligomers used in our experiments may have

unique characteristics that make them more amenable to internalisation and more toxic. For example, hydrophobic regions are exposed in oligomers, which have been shown to affect the affinity with which A β 42 oligomers bind to cellular membranes [86,87]. In contrast, mature fibrils, and most likely the sonicated species we have generated, are highly ordered and stable with the majority of their hydrophobic surfaces buried within the fibre.

Together, our data strongly suggest that conformation and potential for self-assembly rather than size influence A β O-mediated internalisation and neurotoxicity. Despite sharing a similar size to A β O, A β Son are not as readily internalised and are not toxic. Oligomers have a propensity for further self-assembly into mature fibrils using available monomers for elongation, whereas fibrils and sonicated fibrils are already mostly fully assembled. We propose that A β O are more toxic because they are endocytosed more efficiently, and this in turn is dictated by two characteristics: (1) they are structurally distinct from fibrils and sonicated fibrils and (2) oligomers are in a more dynamic state and are continuing to self-assemble. We also show that the toxic effects of A β O are triggered by incubation with cells for only 24 h. These results contribute to our understanding of what makes self-assembled, amyloidogenic proteins toxic.

Methods

Preparation of A β 42

Recombinant A β 42 (NH₂-DAEFRHDSGYEVHHQKLVFFAEDVGSNKGAIIGLMVGGVVIA-COOH) was purchased from rPeptide (CAT# A-1163-2) as 1,1,1,3,3,3-hexafluoro-2-propanol (HFIP) films (>97% purity) with a confirmed molecular mass of 4514.3 Da. 0.2 mg aliquots of peptide were solubilised in 200 μ L HFIP (Merck Life Science UK, Dorset, UK) to dissolve any preformed aggregates. The solution was vortexed for 1 min and sonicated in a 50/60Hz bath sonicator for 5 min. HFIP was dried off using a steady flow of nitrogen gas, and then, 200 μ L of anhydrous dimethyl sulfoxide (DMSO) (Merck Life Science) added and vortexed for 1 min. The solution was sonicated for 1 minute and eluted through a buffer equilibrated 7K MWCO Zeba buffer-exchange column (Thermo Fisher Scientific, Hemel Hempstead, UK) at 4 °C. The protein solution was kept on ice, whilst the absorbance at 280 nm was measured using a NanoDrop spectrophotometer. The concentration was calculated using a molecular coefficient of 1490 $\text{M}^{-1}\cdot\text{cm}^{-1}$; $(A_{280}/1490) \times 10^6$. Solutions were immediately diluted to 50 μM in buffer, and this was taken to be the new working stock. The solution was

incubated at room temperature for 2 h for A β O and at room temperature for 48 h for A β F. For A β Son, the solution was incubated at room temperature for 48 h followed by sonication for 10 min on ice. Solutions were prepared in either HEPES buffer (10 mM HEPES, 50 mM NaCl, 1.6 mM KCl, 2 mM MgCl₂, and 3.5 mM CaCl₂) or 20 mM phosphate buffer (200 mM Na₂HPO₄, 200 mM NaH₂PO₄, diluted to 20 mM with ddH₂O), both at pH 7.4.

Preparation of Alexa Fluor 488-conjugated A β

A β 42 was prepared as described above up to the addition of DMSO. As per the manufacturer's instructions (Life Technologies, Thermo Fisher Scientific), the Alexa Fluor 488 tag was prepared by adding 10 μ L H₂O to an Alexa Fluor TFP ester (kept on ice). This was added to A β 42 in DMSO with 10 μ L 1 M sodium bicarbonate (pH 8.3) and incubated at room temperature for 15 min. From this step onwards, the sample was protected from light using aluminium foil. After this, the usual A β preparation method continued with the Zeba buffer-exchange column. To take into account the absorbance of the dye, the following calculation was used for the concentration of the 488-tagged A β 42 preparation:

$$\text{Protein concentration (M)} = [A_{280} - (A_{494} \times 0.11)] / 1490.$$

For 488-A β O, the solution was incubated for 2 h at room temperature before being added to cells. The preparation was incubated for 48 h at room temperature for 488-A β F, and for 488-A β Son, 488-A β F were sonicated on ice for 10 min.

Transmission electron microscopy

4 μ L of peptide sample was applied to the surface of formvar/carbon film-coated 400-mesh copper grids (Agar Scientific) and allowed to adsorb for 2 min before being blotted dry. The grid was then washed with 4 μ L of Milli-Q-filtered water and blotted dry and negatively stained using 2% (w/v) uranyl acetate for 2 min, blotted and then dried. This was repeated once more, and the grid was left to air dry before being imaged. All grids were examined and imaged using a JEOL JEM1400-Plus TEM at 120 kV, and images were captured using a Gatan OneView 4K camera (Abingdon, UK). FIJI software was used to measure the length of oligomers and sonicated fibrils; three images from three independent preparations were measured.

Circular dichroism

Aliquots of peptide samples (prepared in 20 mM phosphate buffer, pH 7.4) were placed in a 1-mm pathlength quartz cuvette (Hellma). Scans were taken between 180 and 280 nm on a JASCO J715 Spectropolarimeter at 20°C. Three spectra

were averaged for each measurement. Spectral data were converted to molar ellipticity using the following equation: $Mdeg \times \text{Molecular Weight} / (10 \times \text{mg} \cdot \text{mL}^{-1} \times \text{pathlength of cuvette} \times \text{number of amino acids})$.

Western blotting

About 2 μg of A β 42 in 4 \times Laemmli sample buffer (Bio-Rad) containing 1:10 β -mercaptoethanol (BME) was loaded on a 50 μL 10-well 4–20% Mini-PROTEAN TGX Stain-Free gel (Bio-Rad). The gel was run in 1X running buffer (diluted from 10X Tris/Glycine/SDS stock, Bio-Rad) at 100 V. The gel was then transferred on to 0.45- μm nitrocellulose membrane in 1X transfer buffer (diluted from 10X Tris/Glycine stock, Bio-Rad) for 2 h at 25 V. The membrane was incubated with blocking buffer (10% milk in Tris-buffered saline with 0.1% Tween (TBS-T)) at room temperature for 1 h after which 6E10 primary antibody (BioLegend) (1:10,000 dilution in blocking buffer) was applied for overnight at 4°C. The membrane was washed three times with 0.1% TBS-T for 10 min per wash after which the membrane was incubated with horseradish peroxidase (HRP) conjugated anti-mouse secondary antibody (Cell Signalling) (1 : 10 000 dilution in blocking buffer) for 30 min at room temperature. The membrane was washed again three times with 0.1% TBS-T before being incubated with enhanced chemiluminescence (ECL) substrate for 5 minutes. The membrane was developed on CL-Exposure Film (Thermo Fisher).

Cell culture

Rats are housed in a specialised facility under Home Office guidelines and sacrificed using Schedule 1 procedures in accordance with Animals (Scientific Procedures) Act 1986, Amendment Regulations 2012. Primary hippocampal cultures were prepared from either P0 or P1 rats. Initially, the hippocampus was dissected in ice-cold Hanks' Balanced Salt Solution (HBSS) containing 0.1 M HEPES. It was then washed in prewarmed basal medium eagle (BME) (Gibco) containing 0.5% glucose, 2% fetal bovine serum (FBS), 1 mM Na-pyruvate, 0.01 M HEPES (pH 7.35), penicillin/streptomycin, 1% B27 supplement and 1% GlutaMAX. The hippocampus was titrated using a 1-ml pipette until the tissue was fully dissociated and finally diluted further with the BME-supplemented media. Approximately 40,000 cells were plated on poly-D-lysine (20 $\mu\text{g} \cdot \text{mL}^{-1}$) and laminin (20 $\mu\text{g} \cdot \text{mL}^{-1}$) precoated coverslips and incubated at 37 °C and 5% CO₂. After 3–5 days of incubation, the cells were treated with 3.25 μM cytosine arabinoside to stop astrocyte proliferation. Cells were used in experiments 10–14 days after plating.

ReadyProbes cell viability assay

A β 42 was prepared in 10 mM HEPES as described above and incubated at room temperature for 2 hours for A β O,

48 hours for A β F, and fibres were sonicated for 10 minutes on ice for A β Son. Each preparation was incubated with rat primary hippocampal cultures at a final concentration of 10 μM . After incubation with the peptide for the required amount of time, one drop of each ReadyProbes reagent (Life Technologies) was added to the wells. The NucBlue live reagent (excitation/emission at 360 and 460 nm, respectively) stains the nuclei of all cells. The NucGreen dead reagent (excitation/emission at 504 and 523 nm, respectively) stains only the nuclei of dead cells with compromised plasma membranes. Cells were incubated for 15 minutes with the reagents and then imaged using a Zeiss CO widefield microscope using the DAPI and FITC filters. 4–6 regions of interest were imaged per well, and the percentage of dead cells was calculated as the number of green cells in the entire blue-stained population. Astrocytes in the cultures were not counted. The experiment was repeated 3 independent times.

For experiments testing whether A β O internalisation is necessary to mediate cytotoxicity, cells were treated with 10 μM A β O for increasing lengths of time before being replaced with fresh, A β -free media. Cells were incubated for a total of 7 days before using the ReadyProbes assay to measure cytotoxicity.

References

- Selkoe DJ and Hardy J (2016) The amyloid hypothesis of Alzheimer's disease at 25 years. *EMBO Mol Med* **8**, 595–608.
- Benilova I, Karran E and De Strooper B (2012) The toxic A β oligomer and Alzheimer's disease: an emperor in need of clothes. *Nat Neurosci* **15**, 349–357.
- Selkoe DJ (1994) Alzheimer's disease: a central role for amyloid. *J Neuropathol Exp Neurol* **53**, 438–447.
- Serpell LC (2000) Alzheimer's amyloid fibrils: structure and assembly. *Biochim Biophys Acta* **1502**, 16–30.
- Broersen K, Rousseau F and Schymkowitz J (2010) The culprit behind amyloid beta peptide related neurotoxicity in Alzheimer's disease: oligomer size or conformation? *Alzheimers Res Ther* **2**, 12.
- Pike CJ, Burdick D, Walencewicz AJ, Glabe CG and Cotman CW (1993) Neurodegeneration induced by beta-amyloid peptides in vitro: the role of peptide assembly state. *J Neurosci* **13**, 1676–1687.
- Pike CJ, Walencewicz AJ, Glabe CG and Cotman CW (1991) In vitro aging of beta-amyloid protein causes peptide aggregation and neurotoxicity. *Brain Res* **563**, 311–314.
- Williams TL and Serpell LC (2011) Membrane and surface interactions of Alzheimer's A β peptide – insights into the mechanism of cytotoxicity. *FEBS J* **278**, 3905–3917.
- Bitan G, Lomakin A and Teplow DB (2001) Amyloid beta-protein oligomerization: prenucleation interactions

- revealed by photo-induced cross-linking of unmodified proteins. *J Biol Chem* **276**, 35176–35184.
- 10 Bitan G, Vollers SS and Teplow DB (2003) Elucidation of primary structure elements controlling early amyloid beta-protein oligomerization. *J Biol Chem* **278**, 34882–34889.
- 11 Walsh DM, Hartley DM, Kusumoto Y, Fezoui Y, Condron MM, Lomakin A, Teplow DB (1999) Amyloid beta-protein fibrillogenesis. Structure and biological activity of protofibrillar intermediates. *J Biol Chem* **274**, 25945–25952.
- 12 Nelson R, Sawaya MR, Balbirnie M, Madsen AO, Riekel C, Grothe R and Eisenberg D (2005) Structure of the cross-beta spine of amyloid-like fibrils. *Nature* **435**, 773–778.
- 13 Antzutkin ON, Leapman RD, Balbach JJ and Tycko R (2002) Supramolecular structural constraints on Alzheimer's beta-amyloid fibrils from electron microscopy and solid-state nuclear magnetic resonance. *Biochemistry* **41**, 15436–15450.
- 14 Colvin MT, Silvers R, Ni QZ, Can TV, Sergeyev I, Rosay M, Griffin RG (2016) Atomic resolution structure of monomorphic Abeta42 amyloid fibrils. *J Am Chem Soc* **138**, 9663–9674.
- 15 Gremer L, Scholzel D, Schenk C, Reinartz E, Labahn J, Ravelli RBG, Schroder GF (2017) Fibril structure of amyloid-beta(1–42) by cryo-electron microscopy. *Science* **358**, 116–119.
- 16 Kollmer M, Close W, Funk L, Rasmussen J, Bsoul A, Schierhorn A, Fandrich M (2019) Cryo-EM structure and polymorphism of Abeta amyloid fibrils purified from Alzheimer's brain tissue. *Nat Commun* **10**, 4760.
- 17 Schmidt M, Rohou A, Lasker K, Yadav JK, Schiene-Fischer C, Fandrich M and Grigorieff N (2015) Peptide dimer structure in an Abeta(1–42) fibril visualized with cryo-EM. *Proc Natl Acad Sci U S A* **112**, 11858–11863.
- 18 Walti MA, Ravotti F, Arai H, Glabe CG, Wall JS, Bockmann A, Riek R (2016) Atomic-resolution structure of a disease-relevant Abeta(1–42) amyloid fibril. *Proc Natl Acad Sci U S A* **113**, E4976–4984.
- 19 Bezprozvanny I (2009) Amyloid goes global. *Sci Signal* **2**, pe16.
- 20 Meyer-Luehmann M, Spires-Jones TL, Prada C, Garcia-Alloza M, de Calignon A, Rozkalne A, Hyman BT (2008) Rapid appearance and local toxicity of amyloid-beta plaques in a mouse model of Alzheimer's disease. *Nature* **451**, 720–724.
- 21 De Strooper B and Karran E (2016) The cellular phase of Alzheimer's disease. *Cell* **164**, 603–615.
- 22 Hardy JA and Higgins GA (1992) Alzheimer's disease: the amyloid cascade hypothesis. *Science* **256**, 184–185.
- 23 McLean CA, Cherny RA, Fraser FW, Fuller SJ, Smith MJ, Beyreuther K, Masters CL (1999) Soluble pool of Abeta amyloid as a determinant of severity of neurodegeneration in Alzheimer's disease. *Ann Neurol* **46**, 860–866.
- 24 Amar F, Sherman MA, Rush T, Larson M, Boyle G, Chang L, Lesne SE (2017) The amyloid-beta oligomer Abeta*56 induces specific alterations in neuronal signaling that lead to tau phosphorylation and aggregation. *Sci Signal* **10**, 1–14.
- 25 Deshpande A, Mina E, Glabe C and Busciglio J (2006) Different conformations of amyloid beta induce neurotoxicity by distinct mechanisms in human cortical neurons. *J Neurosci* **26**, 6011–6018.
- 26 Ladiwala AR, Litt J, Kane RS, Aucoin DS, Smith SO, Ranjan S, Tessier PM (2012) Conformational differences between two amyloid beta oligomers of similar size and dissimilar toxicity. *J Biol Chem* **287**, 24765–24773.
- 27 Lambert MP, Barlow AK, Chromy BA, Edwards C, Freed R, Liosatos M, Klein WL (1998) Diffusible, nonfibrillar ligands derived from Abeta1–42 are potent central nervous system neurotoxins. *Proc Natl Acad Sci U S A* **95**, 6448–6453.
- 28 Lesne SE, Sherman MA, Grant M, Kuskowski M, Schneider JA, Bennett DA and Ashe KH (2013) Brain amyloid-beta oligomers in ageing and Alzheimer's disease. *Brain* **136** (Pt 5), 1383–1398.
- 29 Shankar GM, Bloodgood BL, Townsend M, Walsh DM, Selkoe DJ and Sabatini BL (2007) Natural oligomers of the Alzheimer amyloid-beta protein induce reversible synapse loss by modulating an NMDA-type glutamate receptor-dependent signaling pathway. *J Neurosci* **27**, 2866–2875.
- 30 Shankar GM, Li S, Mehta TH, Garcia-Munoz A, Shepardson NE, Smith I, Selkoe DJ (2008) Amyloid-beta protein dimers isolated directly from Alzheimer's brains impair synaptic plasticity and memory. *Nat Med* **14**, 837–842.
- 31 Townsend M, Shankar GM, Mehta T, Walsh DM and Selkoe DJ (2006) Effects of secreted oligomers of amyloid beta-protein on hippocampal synaptic plasticity: a potent role for trimers. *J Physiol* **572** (Pt 2), 477–492.
- 32 Lashuel HA. (2005) Membrane Permeabilization: A Common Mechanism in Protein-Misfolding Diseases. *Science of Aging Knowledge Environment* **2005**, pe28.
- 33 Williams TL, Urbanc B, Marshall KE, Vadukul DM, Jenkins AT and Serpell LC (2015) Europium as an inhibitor of Amyloid-beta(1–42) induced membrane permeation. *FEBS Lett* **589**, 3228–3236.
- 34 Liu RQ, Zhou QH, Ji SR, Zhou Q, Feng D, Wu Y and Sui SF (2010) Membrane localization of beta-amyloid 1–42 in lysosomes: a possible mechanism for lysosome labilization. *J Biol Chem* **285**, 19986–19996.
- 35 Marshall KE, Vadukul DM, Staras K and Serpell LC (2020) Misfolded amyloid-beta-42 impairs the

- endosomal-lysosomal pathway. *Cell Mol Life Sci* 1–13. <https://doi.org/10.1007/s00018-020-03464-4>.
- 36 Nixon RA and Cataldo AM (2006) Lysosomal system pathways: genes to neurodegeneration in Alzheimer's disease. *J Alzheimers Dis* **9** (3 Suppl), 277–289.
 - 37 Soura V, Stewart-Parker M, Williams TL, Ratnayaka A, Atherton J, Gorringe K, Serpell LC (2012) Visualization of co-localization in Abeta42-administered neuroblastoma cells reveals lysosome damage and autophagosome accumulation related to cell death. *Biochem J* **441**, 579–590.
 - 38 Bayer TA and Wirths O (2010) Intracellular accumulation of amyloid-Beta – a predictor for synaptic dysfunction and neuron loss in Alzheimer's disease. *Front Aging Neurosci* **2**, 8.
 - 39 Kienlen-Campard P, Miolet S, Tasiaux B and Octave JN (2002) Intracellular amyloid-beta 1–42, but not extracellular soluble amyloid-beta peptides, induces neuronal apoptosis. *J Biol Chem* **277**, 15666–15670.
 - 40 Maina MB, Bailey LJ, Doherty AJ and Serpell LC (2018) The involvement of Abeta42 and tau in nucleolar and protein synthesis machinery dysfunction. *Front Cell Neurosci* **12**, 220.
 - 41 Kaye R, Head E, Sarsoza F, Saing T, Cotman CW, Nuclea M, Glabe CG (2007) Fibril specific, conformation dependent antibodies recognize a generic epitope common to amyloid fibrils and fibrillar oligomers that is absent in prefibrillar oligomers. *Mol Neurodegener* **2**, 18.
 - 42 Verma M, Vats A and Taneja V (2015) Toxic species in amyloid disorders: oligomers or mature fibrils. *Ann Indian Acad Neurol* **18**, 138–145.
 - 43 Walsh DM, Klyubin I, Fadeeva JV, Rowan MJ and Selkoe DJ (2002) Amyloid-beta oligomers: their production, toxicity and therapeutic inhibition. *Biochem Soc Trans* **30**, 552–557.
 - 44 Marshall KE, Vadukul DM, Dahal L, Theisen A, Fowler MW, Al-Hilaly Y, Serpell LC (2016) A critical role for the self-assembly of Amyloid-beta1-42 in neurodegeneration. *Sci Rep* **6**, 30182.
 - 45 Cohen SI, Vendruscolo M, Dobson CM and Knowles TP (2011) Nucleated polymerisation in the presence of pre-formed seed filaments. *Int J Mol Sci* **12**, 5844–5852.
 - 46 Tornquist M, Michaels TCT, Sanagavarapu K, Yang X, Meisl G, Cohen SIA, Linse S (2018) Secondary nucleation in amyloid formation. *Chem Commun (Camb)* **54**, 8667–8684.
 - 47 Hatami A, Albay R 3rd, Monjazebe S, Milton S and Glabe C (2014) Monoclonal antibodies against Abeta42 fibrils distinguish multiple aggregation state polymorphisms in vitro and in Alzheimer disease brain. *J Biol Chem* **289**, 32131–32143.
 - 48 Jin S, Kedia N, Illes-Toth E, Haralampiev I, Prisner S, Herrmann A, Bieschke J (2016) Amyloid-beta(1–42) Aggregation initiates its cellular uptake and cytotoxicity. *J Biol Chem* **291**, 19590–19606.
 - 49 Lai AY and McLaurin J (2010) Mechanisms of amyloid-Beta Peptide uptake by neurons: the role of lipid rafts and lipid raft-associated proteins. *Int J Alzheimers Dis* **2011**, 548380.
 - 50 Li HQ, Chen C, Dou Y, Wu HJ, Liu YJ, Lou HF, Duan S (2013) P2Y4 receptor-mediated pinocytosis contributes to amyloid beta-induced self-uptake by microglia. *Mol Cell Biol* **33**, 4282–4293.
 - 51 Yang WN, Ma KG, Chen XL, Shi LL, Bu G, Hu XD, Qian YH (2014) Mitogen-activated protein kinase signaling pathways are involved in regulating alpha7 nicotinic acetylcholine receptor-mediated amyloid-beta uptake in SH-SY5Y cells. *Neuroscience* **278**, 276–290.
 - 52 Yu C, Nwabuisi-Heath E, Laxton K and Ladu MJ (2010) Endocytic pathways mediating oligomeric Abeta42 neurotoxicity. *Mol Neurodegener* **5**, 19.
 - 53 Zheng L, Calvo-Garrido J, Hallbeck M, Hultenby K, Marcusson J, Cedazo-Minguez A and Terman A (2013) Intracellular localization of amyloid-beta peptide in SH-SY5Y neuroblastoma cells. *J Alzheimers Dis* **37**, 713–733.
 - 54 Harte NP, Klyubin I, McCarthy EK, Min S, Garrahy SA, Xie Y, Mok KH (2015) Amyloid oligomers and mature fibrils prepared from an innocuous protein cause diverging cellular death mechanisms. *J Biol Chem* **290**, 28343–28352.
 - 55 Lee YJ, Savtchenko R, Ostapchenko VG, Makarava N and Baskakov IV (2011) Molecular structure of amyloid fibrils controls the relationship between fibrillar size and toxicity. *PLoS One* **6**, e20244.
 - 56 Xue WF, Hellewell AL, Gosal WS, Homans SW, Hewitt EW and Radford SE (2009) Fibril fragmentation enhances amyloid cytotoxicity. *J Biol Chem* **284**, 34272–34282.
 - 57 Harper JD, Wong SS, Lieber CM and Lansbury PT (1997) Observation of metastable Abeta amyloid protofibrils by atomic force microscopy. *Chem Biol* **4**, 119–125.
 - 58 Ahmed M, Davis J, Aucoin D, Sato T, Ahuja S, Aimoto S, Smith SO (2010) Structural conversion of neurotoxic amyloid-beta(1–42) oligomers to fibrils. *Nat Struct Mol Biol* **17**, 561–567.
 - 59 Pujol-Pina R, Vilaprinyo-Pascual S, Mazzucato R, Arcella A, Vilaseca M, Orozco M and Carulla N (2015) SDS-PAGE analysis of Abeta oligomers is disserving research into Alzheimer's disease: appealing for ESI-IM-MS. *Sci Rep* **5**, 14809.
 - 60 Yu L, Edalji R, Harlan JE, Holzman TF, Lopez AP, Labkovsky B, Olejniczak ET (2009) Structural characterization of a soluble amyloid beta-peptide oligomer. *Biochemistry* **48**, 1870–1877.

- 61 Cheon M, Chang I, Mohanty S, Luheshi LM, Dobson CM, Vendruscolo M and Favrin G (2007) Structural reorganisation and potential toxicity of oligomeric species formed during the assembly of amyloid fibrils. *PLoS Comput Biol* **3**, 1727–1738.
- 62 Stroud JC, Liu C, Teng PK and Eisenberg D (2012) Toxic fibrillar oligomers of amyloid-beta have cross-beta structure. *Proc Natl Acad Sci U S A* **109**, 7717–7722.
- 63 Stathopoulos PB, Scholz GA, Hwang YM, Rumfeldt JA, Lepock JR and Meiering EM (2004) Sonication of proteins causes formation of aggregates that resemble amyloid. *Protein Sci* **13**, 3017–3027.
- 64 Chimon S, Shaibat MA, Jones CR, Calero DC, Aizezi B and Ishii Y (2007) Evidence of fibril-like beta-sheet structures in a neurotoxic amyloid intermediate of Alzheimer's beta-amyloid. *Nat Struct Mol Biol* **14**, 1157–1164.
- 65 Parthasarathy S, Inoue M, Xiao Y, Matsumura Y, Nabeshima Y, Hoshi M and Ishii Y (2015) Structural insight into an Alzheimer's brain-derived spherical assembly of amyloid beta by solid-state NMR. *J Am Chem Soc* **137**, 6480–6483.
- 66 Lendel C, Bjerring M, Dubnovitsky A, Kelly RT, Filippov A, Antzutkin ON, Hard T (2014) A hexameric peptide barrel as building block of amyloid-beta protofibrils. *Angew Chem Int Ed Engl* **53**, 12756–12760.
- 67 Ciudad S, Puig E, Botzanowski T, Meigooni M, Arango AS, Do J, Carulla N (2020) Abeta(1–42) tetramer and octamer structures reveal edge conductivity pores as a mechanism for membrane damage. *Nat Commun* **11**, 3014.
- 68 Jang H, Arce FT, Capone R, Ramachandran S, Lal R and Nussinov R (2009) Misfolded amyloid ion channels present mobile beta-sheet subunits in contrast to conventional ion channels. *Biophys J* **97**, 3029–3037.
- 69 Quist A, Doudevski I, Lin H, Azimova R, Ng D, Frangione B, Lal R (2005) Amyloid ion channels: a common structural link for protein-misfolding disease. *Proc Natl Acad Sci U S A* **102**, 10427–10432.
- 70 Glabe CG (2008) Structural classification of toxic amyloid oligomers. *J Biol Chem* **283**, 29639–29643.
- 71 Bystrenova E, Bednarikova Z, Barbalinardo M, Albonetti C, Valle F and Gazova Z (2019) Amyloid fragments and their toxicity on neural cells. *Regen Biomater* **6**, 121–127.
- 72 Chafekar SM, Baas F and Scheper W (2008) Oligomer-specific Abeta toxicity in cell models is mediated by selective uptake. *Biochim Biophys Acta* **1782**, 523–531.
- 73 Dahlgren KN, Manelli AM, Stine WB Jr, Baker LK, Krafft GA and LaDu MJ (2002) Oligomeric and fibrillar species of amyloid-beta peptides differentially affect neuronal viability. *J Biol Chem* **277**, 32046–32053.
- 74 He Y, Zheng MM, Ma Y, Han XJ, Ma XQ, Qu CQ and Du YF (2012) Soluble oligomers and fibrillar species of amyloid beta-peptide differentially affect cognitive functions and hippocampal inflammatory response. *Biochem Biophys Res Commun* **429**, 125–130.
- 75 Paranjape GS, Gouwens LK, Osborn DC and Nichols MR (2012) Isolated amyloid-beta(1–42) protofibrils, but not isolated fibrils, are robust stimulators of microglia. *ACS Chem Neurosci* **3**, 302–311.
- 76 Morten IJ, Gosal WS, Radford SE and Hewitt EW (2007) Investigation into the role of macrophages in the formation and degradation of beta2-microglobulin amyloid fibrils. *J Biol Chem* **282**, 29691–29700.
- 77 Gouras GK, Tampellini D, Takahashi RH and Capetillo-Zarate E (2010) Intraneuronal beta-amyloid accumulation and synapse pathology in Alzheimer's disease. *Acta Neuropathol* **119**, 523–541.
- 78 Grundke-Iqbal I, Iqbal K, George L, Tung YC, Kim KS and Wisniewski HM (1989) Amyloid protein and neurofibrillary tangles coexist in the same neuron in Alzheimer disease. *Proc Natl Acad Sci U S A* **86**, 2853–2857.
- 79 Wirths O, Multhaup G, Czech C, Feldmann N, Blanchard V, Tremp G, Bayer TA (2002) Intraneuronal APP/A beta trafficking and plaque formation in beta-amyloid precursor protein and presenilin-1 transgenic mice. *Brain Pathol* **12**, 275–286.
- 80 Domert J, Rao SB, Agholme L, Brorsson AC, Marcusson J, Hallbeck M and Nath S (2014) Spreading of amyloid-beta peptides via neuritic cell-to-cell transfer is dependent on insufficient cellular clearance. *Neurobiol Dis* **65**, 82–92.
- 81 Kumari S, Mg S and Mayor S (2010) Endocytosis unplugged: multiple ways to enter the cell. *Cell Res* **20**, 256–275.
- 82 Rejman J, Oberle V, Zuhorn IS and Hoekstra D (2004) Size-dependent internalization of particles via the pathways of clathrin- and caveolae-mediated endocytosis. *Biochem J* **377** (Pt 1), 159–169.
- 83 Tipping KW, Karamanos TK, Jakhria T, Iadanza MG, Goodchild SC, Tuma R, Radford SE (2015) pH-induced molecular shedding drives the formation of amyloid fibril-derived oligomers. *Proc Natl Acad Sci U S A* **112**, 5691–5696.
- 84 Bode DC, Freeley M, Nield J, Palma M and Viles JH (2019) Amyloid-beta oligomers have a profound detergent-like effect on lipid membrane bilayers, imaged by atomic force and electron microscopy. *J Biol Chem* **294**, 7566–7572.
- 85 Bode DC, Baker MD and Viles JH (2017) Ion channel formation by amyloid-beta42 oligomers but not amyloid-beta40 in cellular membranes. *J Biol Chem* **292**, 1404–1413.

- 86 Evangelisti E, Cascella R, Becatti M, Marrazza G, Dobson CM, Chiti F, Cecchi C (2016) Binding affinity of amyloid oligomers to cellular membranes is a generic indicator of cellular dysfunction in protein misfolding diseases. *Sci Rep* **6**, 32721.
- 87 Mannini B, Mulvihill E, Sgromo C, Cascella R, Khodarahmi R, Ramazzotti M, Chiti F (2014) Toxicity of protein oligomers is rationalized by a function combining size and surface hydrophobicity. *ACS Chem Biol* **9**, 2309–2317.

Supporting information

Additional supporting information may be found online in the Supporting Information section at the end of the article.

Fig S1. Quantification of fluorescence intensity in neurons over time treated with Alexa fluor 488 tagged A β O, A β F or A β SoN. Values are taken from figure 4b to display a comparison of the different species.